

Using Pad-Stripped Acausally Filtered Strong-Motion Data

By David M. Boore, Aida Azari Sisi, and Sinan Akkar

Abstract

Most strong-motion data processing involves acausal low-cut filtering, which requires the addition of sometimes lengthy zero pads to the data. These padded sections are commonly removed by organizations supplying data, but this can lead to incompatibilities in measures of ground motion derived in the usual way from the padded and the pad-stripped data. One way around this is to use the correct initial conditions in the pad-stripped time series when computing displacements, velocities, and oscillator response. Another way of ensuring compatibility is to use post-processing of the pad-stripped acceleration time series. Using 1357 three-component records from the Turkish strong-motion database, we show that the procedures used by two organizations---ITACA (Italian Accelerometric Archive) and PEER NGA (Pacific Earthquake Engineering Research Center Next Generation Attenuation)—lead to little bias and distortion of derived seismic-intensity measures.

Introduction

An essential part of most processing of strong-motion data is low-cut (high-pass) filtering to remove the long-period noise that is ubiquitous in both analog and digital data (*e.g.*, Boore and Bommer, 2005). Acausal (zero-phase) filtering is used most commonly (to avoid distortions associated with the phase shift of causal filter (Boore and Akkar, 2003)), and this requires adding zero pads to the time series before filtering in order to avoid wrap-around effects due to the filter transients and to include the effects of the filter transients when performing operations such as integration to obtain displacements and in the computation of response spectra (*e.g.*, Boore, 2005). After filtering, it is common for some organizations providing data to strip off the padded portions of the data (we call the resulting acceleration time series “pad-stripped accelerations”), and thus processed strong-motion data made available to the public rarely includes these padded and filtered sections of the processed data. One reason for doing so

might be because plots of the padded and filtered accelerations would appear to have a long section of zero motion before the arrival of the shaking, and users might be tempted to remove this section of the time series. Doing so, however, may lead to distortions in quantities such as peak displacements and oscillator response derived from the truncated time series.

Different organizations have various ways of dealing with the pad-stripped data. The ground-motion intensity measures (GMIMs) such as peak velocity, peak displacement, and response spectra provided to the public by National Strong-Motion Program of the U.S. Geological Survey are obtained from the processed data before stripping off the zero pads (C. Stephens, oral commun., 2011). This means that those measures, as well as the velocity and displacement time series, might be incompatible with the pad-stripped acceleration time series that are distributed to the public in the sense that those quantities often cannot be obtained by integration of the distributed acceleration time series or using it to compute response spectra. As we will show, compatibility can be assured by providing initial values of displacement and velocity for the pad-stripped accelerations and oscillator response, but this is not done by any data-providing organization of which we are aware. One purpose of this article is to demonstrate that providing a small amount of additional data would ensure compatibility of the pad-stripped accelerations with the other quantities provided by the organization; this is discussed in the next section of the article.

Several organizations deal with the compatibility issue by first processing the accelerations in the usual way (zero-padding and filtering). Instead of deriving intensity measures from these processed accelerations, however, a type of post-processing is applied to the pad-stripped accelerations. For the two organizations considered in this article (ITACA and PEER NGA), this post processing involves fitting polynomials to the velocities and/or displacements obtained from the pad-stripped processed accelerations and using these to adjust the pad-stripped accelerations. The intensity measures are derived from these adjusted, pad-stripped accelerations, and thus the intensity measures and the velocity and displacement time series are compatible with the post-processed pad-stripped accelerations. This procedure seems unnecessarily complex if the standard ground-motion intensity measures (peak acceleration (PGA), peak velocity (PGV), peak displacement (PGD) and elastic response spectra) are desired,

as these measures could have been obtained from the padded and filtered acceleration time series that is a part of the processing scheme. The second purpose of our article is to evaluate whether the post-processing method used by ITACA and PEER NGA has introduced biases or distortions in the intensity measures. This is an important topic, because the intensity measures used for such things as deriving ground-motion prediction equations are often those from organizations providing data obtained using post-processing methods. The bulk of the article is devoted to this topic.

Using Initial Conditions with Pad-Stripped Filtered Accelerations

The processing methods discussed in this article are illustrated with the EW component of motion recorded by an analog Kinematics SMA-1 strong-motion accelerograph at station Dinar-Meteorology Station ($R_{HYP} = 5 \text{ km}$, $V_{S30} = 198 \text{ m/s}$) from the 01 October 1995 Dinar earthquake (M 6.4). The record is from the Turkish database (Akkar *et al.*, 2010), and additional information about the station and the earthquake can be found in Anderson *et al.* (2001). The record was padded with zeros and then filtered with an acausal bandpass with corner frequencies of 0.15 Hz and 30 Hz (these values are from the Turkish database). Figure 1 is a plot of the filtered acceleration time series, with and without pads. No pre-event filter transient is obvious in the top graph, which illustrates our previous comment about the appearance of padded and filtered accelerations. Such a transient exists, however, as is clearly shown when the ordinate scale is expanded greatly (Figure 1b). Even though relatively small in amplitude, these transients are important in the derivation of velocity, displacement, and response spectra, but they are not available in the pad-stripped data. Ignoring the filter transient and integrating pad-stripped accelerations with the common assumption that the initial velocity and displacements are 0.0 usually leads to long-period errors appearing as a drift in the displacement time series (Figure 2). In addition, computing response spectra from the pad-stripped acceleration time series, again with the common assumption of 0.0 initial conditions, leads to significant differences at long period relative to the response spectrum obtained from the padded accelerations (which we consider to be the correct response spectrum for the given choice of filter corner frequencies), as shown in Figure 3.

Distributing the padded and filtered acceleration time series and quantities such as GMIMs and velocity and displacement time series derived from the padded and filtered acceleration time series clearly avoids compatibility problems. But as noted before, many organizations provide only pad-stripped data. It is true that the padding often amounts to more than the length of the pad-stripped time series and the amplitudes of the filter transients in the padded sections can be quite small. For this reason users might not understand why they should use portions of the record with apparently inconsequential motions. It would be all right to skip these zero pad sections for many purposes (as shown by the good agreement in Figure 3 of response spectra from padded and pad-stripped data for periods less than 6 s). But it is possible to provide a small amount of additional data that allows pad-stripped data to be used to calculate velocity and displacement time series and response spectra without distortions. This extra information is the velocity and displacement at the first point of the pad-stripped data, as well as the velocity and displacement oscillator response at the first pad-stripped time point (for each oscillator period and damping). These are sufficient for the computation of undistorted ground-motion intensity measures, as is obvious from the algorithms used for the ground-motion intensity measure calculations. These calculations are done on a time-step by time-step basis, using initial conditions at the start of each time step to calculate the values for the next time step. We now show that this works.

Figure 4 is a blowup of the velocity and displacement traces in the vicinity of the initial point of the pad-stripped data. Using the values of the velocity and displacement as initial conditions in the integration of the pad-stripped acceleration (using a step-by-step application of the trapezoidal integration method) gives the displacement time series shown in Figure 2. The match with the displacements obtained from integration of the padded acceleration time series is essentially perfect (within computational error), as it must be, given the integration method. For computing response spectra we follow Nigam and Jennings (1969). Their method uses initial oscillator velocity and displacement at the beginning of a time interval to predict the oscillator response at the next time step (assuming a linear dependence of acceleration over the time interval of interest), and this procedure is used sequentially through the length of the acceleration time series. The peak of the resulting oscillator-response time series provides one point on the response spectrum curve. As for the computation of peak displacement and peak velocity, we

can compute response spectra from the pad-stripped acceleration time series if the initial velocities and displacement are provided for each oscillator period and damping. For illustration, we show the response of a 5%-damped, 60 s oscillator by the thick curve in Figure 5 (we chose 60 s so that the distortion in the oscillator response is obvious). We obtained the initial oscillator velocity and displacement at $t = 0$ s and used them to compute the oscillator response shown by the thin solid curve in Figure 5 (for comparison, the oscillator response assuming zero initial conditions is shown by the thin dashed curve). Clearly the proper initial conditions lead to the correct response. But this is true only for the portion of the time series corresponding to the original acceleration time series (between the two vertical lines); beyond that point, the filter transient is missing and therefore the response is erroneous. Fortunately, the peak oscillator response is usually in the portion of actual shaking, and therefore the later distortions in the time-domain response of the oscillator will not generally lead to an underestimation of the oscillator response. The peak responses for the two initial conditions are 22.84 cm at 14.92 s for the 0.0 initial conditions and -9.67 cm at 4.35 s for the correct initial conditions; these are also plotted in Figure 3 as part of the response spectrum comparisons. Repeating this procedure for all oscillator periods would give the same response spectrum from the pad-stripped acceleration time series as for the padded acceleration time series, with less information being stored.

The amount of added information is not necessarily onerous compared to the storage requirements of the pads, particularly for records processed with long-period filter cutoffs. For example, the current NGA database contains 1113 GMIMs (response spectra at 111 periods and 10 damping values per period, plus PGA, PGV, and PGD). Thus compatibility could be ensured by providing 2226 additional values to the pad-stripped acceleration time series. This seems like a large number of values, but 6000 leading zeros are required for a 200 sample-per-second record filtered at 10 s, with a low-cut filter going as f^8 at low frequency (Boore, 2005). In addition, if the response for only one value of damping was desired, the number of additional data would be reduced by almost a factor of ten (225 values for 111 periods and PGA, PGV, and PGD).

Using pad-stripped data with the correct initial conditions will probably not work for nonlinear oscillator response, for which the response has memory that is not captured by the initial velocity

and displacement; investigating this is beyond the scope of this article, but we note that this caveat also applies to the post-processing methods discussed next.

Post-Processing of Pad-Stripped Filtered Accelerations

As noted in the introduction, at least two organizations that provide large databases of strong-motion data use acausal filtering, but then strip off the padded portions after filtering and apply a post-processing method to ensure compatibility of the resulting acceleration, velocity, and displacement time series and the ground-motion intensity measures derived from these time series. Because their methods are available to us and because their results are widely distributed, we consider the procedures of these two organizations---ITACA, which is the principal Italian strong-motion data provider, and what we call PEER NGA, which has produced a global strong-motion database for use in developing the Pacific Earthquake Engineering Research (PEER) Center Next Generation Attenuation (NGA) ground-motion prediction equations (GMPEs). The first set of PEER NGA GMPEs was published in 2008, and these are now being revised, using an updated and expanded database (see Chiou *et al.*, 2008, for a description of the database used for the 2008 GMPEs).

The ITACA and PEER NGA Post-Processing Procedures

Simplified flow charts for the ITACA and the PEER NGA post-processing procedures are given in Figures 6 and 7. These flow charts were developed from Pacor *et al.* (2011) for ITACA, based on Paolucci *et al.* (2011), as well as from written communications with people who developed and/or are using the procedures. This includes F. Pacor (for ITACA) and N. Abrahamson, R. Darragh and W. Silva (for PEER NGA). In addition, we have the software used by ITACA and the core program used by PEER NGA (see the Data and Resources section), and the flow charts used this information. The basic difference between the ITACA and the PEER NGA procedures is that the former does linear detrending of the velocity and displacements obtained from the pad-stripped data, whereas PEER NGA fits a 6th order polynomial (in most cases) to the displacements. ITACA then obtains a corrected acceleration

time series by double differentiation of the detrended displacement time series, while PEER NGA subtracts the analytical second derivative of the fitted polynomial from the acceleration time series (in order for this to be compatible with the velocity and displacement time series, which are derived assuming zero initial conditions, the coefficients of the 0th and 1st order terms in the polynomial are constrained to be 0.0, in effect removing the ambiguity of the constants of integration).

Evaluation of post-processing methods

Although the developers of the ITACA and the PEER NGA post-processing procedures undoubtedly checked their results with at least a few records (e.g, Paolucci *et al.*, 2011, show comparisons for three records, but qualitatively describe results from a larger number of records), we wanted to do a comprehensive and quantitative evaluation of the procedures, for which we needed a database containing a large number of unprocessed data. Because it is readily available to us, we used data from the recently compiled Turkish strong-motion database (see the Data and Resources section). These data are almost entirely digital data for earthquakes from **M** 2.8 to 7.6, recorded at distances of 0 to 200 km. We used 2714 horizontal-component time series, and 1357 vertical-component time series. Only 28 analog 3-component recordings were used. Most of the time series are sampled at 200 points/s. None of the records were classified as “late triggers”, as defined by the ITACA procedure. We first processed each record using the procedure given in the flow chart in Figure 8, using filter corner frequencies from the Turkish strong-motion database and pad lengths from Converse and Brady (1992) (as given by equation (1) in Boore (2005)). This provided what we call “reference” measures of ground-motion intensity measures, including PGA, PGV, PGD, and 5%-damped PSA (pseudo-absolute response spectral acceleration). The filter corner frequencies were chosen on a record-by-record basis as part of the uniform processing of the Turkish database. We then processed the uncorrected time series using the ITACA and the PEER NGA procedures. We used the Matlab program written by R. Puglia for the ITACA processing. We could not obtain the software being used by the contractor doing the processing for PEER NGA, so we wrote our own software, incorporating the essential correction subroutine written by N. Abrahamson. We verified that our results compared well with those done at our request by the contractor for two test records.

A comparison of the displacements obtained by the three procedures for the Dinar example is shown in Figure 9. Clearly, the comparison is quite favorable. To provide a more detailed comparison, we computed ratios of PGA, PGV, PGD, and 5%-damped PSA (for many periods) computed by ITACA and PEER NGA relative to the reference measures. We made plots of these ratios for subsets of magnitudes and distances, but as the plots were quite similar, we combined the ratios for all magnitudes and distances into a single figure. The ratios for horizontal and vertical components are given in Figures 10 and 11, respectively. For each figure the ITACA/Reference results are given in the left column and the PEER NGA/Reference results are given in the right column. The ratios are plotted against oscillator period in the top row and against oscillator period divided by the low-cut filter corner period used in processing each record in the bottom row of graphs. One problem with the ratio plots is that attention is drawn to the outliers, whereas the bulk of the ratios plot near unity. The outliers are associated with low values of PGA, as shown in the histogram in Figure 12; the most extreme outliers belong to analog recordings, for which we have found somewhat more sensitivity to the processing method than for digital records. To see better where the bulk of the ratios lie, we have included the 5, 50, and 95 percentile curves in each graph in Figures 10 and 11. These curves show that ratios are quite close to unity (with 90% of the ratios generally falling well within 10% of unity), but with some period dependence. (Not shown here is that for the small number of analog recordings, the 90% range is within 10% of unity for periods less than 1 s but is close to or somewhat larger than 10% of unity for longer periods.) Interestingly, the ratios become particularly close to unity for periods between about 0.1 and 1 s, a range of importance to engineers and also a range corresponding to much of the frequency content of the ground motion. When the normalized period increases beyond about 0.5 the fluctuations in ratios increases, emphasizing the fact that the recordings should only be used up to a fraction of their low-cut filter cut-off values (Akkar and Bommer, 2006). The ratios are somewhat closer to unity for the PEER NGA processing than the ITACA processing.

A better way to look at the distribution of the ratios, at the expense of not being able to see period dependence quite as clearly as in Figures 10 and 11, is to compute and plot histograms of the ratios for selected periods. This is done in Figures 13 and 14. Those figures show that the

ratios are generally larger for the vertical components than the horizontal components, with the distribution of the ITACA ratios being more skewed and somewhat larger than those from the PEER NGA processing. But overall the bulk of the ratios are close to unity for both procedures.

We are not sure what produces the skewed distributions for the ITACA results, but we think that the skewness for PGA is related to the procedure used to double differentiate the post-processed displacements (it is not due to a front taper that is so long that some of the peak motions are reduced, as we carefully chose the tapers so that this would not be the case). The ITACA procedure uses two passes of a two-point, non-centered difference operator (F. Pacor, written commun., 16 December 2010). To test our conjecture, we applied the double differentiation used in the ITACA processing to displacement time series obtained from the reference acceleration time series (the padded and filtered, non-pad-stripped, time series). Figure 15 shows histograms of the ratios of PGA from the ITACA differentiation procedure to the PGA of the reference time series for horizontal and for vertical components. The distribution is skewed and looks quite similar to those in Figures 13 and 14.

Discussion and Conclusions

Processing of strong-motion data usually involves acausal low-cut filtering. This requires the addition of zero pads to the original time series. Removing these padded portions after filtering can result in incompatibilities and biases in quantities derived from the pad-stripped accelerations, unless special consideration is given to the pad-stripped data. One way of overcoming this incompatibility is to provide the velocity and displacement values at the first time point of the pad-stripped data, for both the ground motions and the oscillator responses (for all oscillator periods and damping). These values can be used as initial conditions to recover the same velocity and displacement time series and response spectrum as derived from the padded and filtered acceleration time series (the TSPP software of Boore (2010) allows for initial conditions in calculating GMIMs). Another way of ensuring compatibility of the information being provided is to use post-processing of the pad-stripped acceleration. This is the approach used by ITACA and by PEER NGA. Because data from these organizations are widely used, and because we were concerned that the post-processing might introduce biases and distortions

in the derived seismic intensity measures, we studied the ratios of the measures from those procedures to those from the padded and filtered time series, using 4071 time series (including both horizontal and vertical components) from the Turkish strong-motion database. We came to the important conclusion that any biases and distortions are small for the vast majority of the records, and thus data from ITACA and PEER NGA can be used with confidence that the post-processing has not affected the bulk of the results.

Compatibility is not an issue if the padded and filtered acceleration time series are used in computations of various measures of ground motion. The reason not to use the complete, padded, time series may be due to a lack of appreciation of the existence of pre-event filter transients and the importance of those transients on derived motions. It may seem as if the very low-level pre-event motions can be discarded with impunity, which is a great temptation when doing such computer-intensive calculations as nonlinear structural response--why include motions that look to be zero as input to the structure? But as we have demonstrated, using incorrect initial conditions as a result of ignoring the filter transients can lead to large distortions in long-period linear oscillator response. This might be even truer for nonlinear oscillator response, for which hysteresis means that it might not be possible to provide correct initial conditions after stripping off the pads. It is also possible that the hysteresis effects will lead to biases in the nonlinear calculations using pad-stripped post-processed acceleration time series, relative to the results obtained from the padded and filtered acceleration time series. The possible importance of the pre-event padded portions of the filtered acceleration time series seems to be overlooked by many nonlinear structural analysis programs. These programs are not designed to use long acceleration time series, as in the case of acausally filtered data, due to memory problems, although this may be a legacy from times when memory limitations were more important. A study should be made using the reference and post-processed pad stripped motions to evaluate whether or not ignoring the pre-event portions of the time series leads to biases in nonlinear response of structural systems. Such a study is beyond the scope of this paper, as it would require many structural parameters to be systematically considered in the statistical analysis.

Data and Resources

The Turkish strong-motion data came from <http://daphne.deprem.gov.tr> (last accessed October, 2011). The padding, filtering, integration to velocity and displacement, and the computation of response spectra used the USDP package (<http://web.ce.metu.edu.tr/~sakkar/usdp.html>, last accessed October, 2011), which is based on the TSPP suite of programs described in Boore (2010) and available from the online software page of www.daveboore.com (last accessed October, 2011). The processing of the pad-stripped records used Norm Abrahamson's Bline03-plot suite of Fortran programs (for the NGA processing), a subroutine for frequency-domain Butterworth filter response from W. Silva, and the Matlab script `Process_Records_ITACA_1_1.m` (for ITACA), written by R. Puglia.

Acknowledgments

We thank Norm Abrahamson for providing his post-processing program, Walt Silva for sharing his subroutine for Butterworth frequency-domain filter response, and Francesca Pacor and Marco Massa for sending us R. Puglia's ITACA processing code and for answering questions about the processing. We thank Bob Darragh and Walt Silva for a number of useful discussions regarding the details of the processing procedures used for the NGA project as well as processing two records provided by us. Discussions with Chris Stephens were very useful. The work to develop the strong-motion database used herein was supported by the SHARE (Seismic Hazard Harmonization in Europe) and NERA (Network of European Research Infrastructures for Earthquake Risk Assessment and Mitigation) projects funded under contracts 226967 and 262330 of the EC-Research Framework Programme FP7, respectively. We are grateful to Dino Bindi, Bob Darragh, John Douglas, Eric Chael, Francesca Pacor, and Chris Stephens for insightful reviews that improved the paper.

References

Akkar, S. and J. J. Bommer (2006). Influence of long-period filter cut-off on elastic spectral displacements, *Earthquake Eng. and Structural Dynamics* **35**, 1145-1165.

- Akkar, S., Z. Çağnan, E. Yenier, Ö. Erdoğan, M.A. Sandıkkaya, and P. Gülkan (2010). The recently compiled Turkish strong-motion database: Preliminary investigation for seismological parameters, *J. Seismology* **14**, 457-479.
- Anderson, J. G., Y. Zeng, and H. Sucuoglu (2001). Analysis of accelerations from the 1 October 1995 Dinar, Turkey, earthquake, *Bull. Seismol. Soc. Am.* **91**, 1433-1445.
- Boore, D. M. (2005). On pads and filters: Processing strong-motion data, *Bull. Seism. Soc. Am.* **95**, 745-750.
- Boore, D. M. (2010). TSPP---A collection of FORTRAN programs for processing and manipulating time series, *U.S. Geological Survey Open-File Report* **2008-1111** (Revision 2.1).
- Boore, D. M. and S. Akkar (2003). Effect of causal and acausal filters on elastic and inelastic response spectra, *Earthq. Eng. and Struct. Dynamics* **32**, 1729-1748.
- Boore, D. M. and J. J. Bommer (2005). Processing of strong-motion accelerograms: Needs, options and consequences, *Soil Dynamics and Earthquake Engineering* **25**, 93-115.
- Chiou, B.S.J., Darragh, R., Gregor, N., and Silva, W. (2008). NGA project strong-motion database, *Earthquake Spectra* **24**, 23-44.
- Converse, A. M. and A. G. Brady (1992). BAP --- Basic strong-motion accelerogram processing software; Version 1.0, *U. S. Geological Survey Open-File Report* **92-296A**, 174p.
- Nigam, N. C. and P. C. Jennings (1969). Calculation of response spectra from strong-motion earthquake records, *Bull. Seismol. Soc. Am.* **59**, 909-922.
- Pacor F., R. Paolucci, G. Ameri, M. Massa, and R. Puglia (2011). Italian strong motion records in ITACA: overview and record processing, *Bull. Earthquake Eng.* **9**, 1741-1759.
- Paolucci, R., F. Pacor, R. Puglia, G. Ameri, C. Cauzzi, and M. Massa (2011). Record processing

in ITACA, the new Italian strong-motion database, in *Earthquake Data in Engineering Seismology: Predictive Models, Data Management, and Networks*, Sinan Akkar, Polat Gülkan, and Torild Van Eck, Editors, Springer, Dordrecht, 99-113.

Contact Information

U.S. Geological Survey

MS 977

345 Middlefield Road

Menlo Park, CA 94025

boore@usgs.gov

(D.M.B.)

Earthquake Engineering Research Center

Middle East Technical University

06800 Ankara, Turkey

aida.sisi@metu.edu.tr

sakkar@metu.edu.tr

(A.A.S. and S.A.)

Figure Captions

Figure 1. The acceleration time series from the Dinar recording of the 1995 Dinar earthquake after padding and filtering with an acausal low-cut filter with a corner frequency of 0.15 Hz. The thin curved line superimposed on the thick line in (a) corresponds to the time series after stripping off the padded portion. The vertical lines in the upper graph show the time limits of the original data. The vertical scale in the lower graph is expanded greatly in order to see the filter transients.

Figure 2. Displacements derived from double integration of the acceleration time series shown in Figure 1. The thick curved line is from the complete padded and filtered acceleration, whereas the dashed curve and the thin curve superimposed on the thick curved line are from integration of the pad-stripped filtered acceleration, with initial conditions for the velocity and displacement of 0.0 and the correct initial conditions, respectively.

Figure 3. Response spectra computed from the unfiltered and filtered data used in the previous figures. The heavy gray curve shows the response spectrum from the time series obtained by stripping off the padded portions of the filtered acceleration time series. For all examples 0.0 was assumed for the initial oscillator displacement and velocity, except for the symbols, which were derived from oscillator time series computed from pad-stripped accelerations with different initial conditions (see text).

Figure 4. An expanded portion of the velocity and displacement time series derived from the padded and filtered acceleration shown in Figure 1. The curves superimposed on the thick curved lines start at the zero time of the original record and show that initial conditions of 0.0 for integration of the pad-stripped acceleration time series are incorrect.

Figure 5. The $T = 60$ s oscillator response for the processed data where the padded portions were retained and were stripped off, with initial conditions as shown in the legend. The thick curved line is from the complete padded and filtered acceleration, whereas the dashed curve and the thin curve superimposed on the thick curved line are from the pad-stripped filtered acceleration with

initial conditions for the oscillator velocity and displacement of 0.0 and the correct initial conditions, respectively. The vertical lines show the extent of the original record before padding; 19.995 s of zeros were added before and after the original time series, and additional zeros were added at the end of the processed time series to allow the run-down of the oscillator response (only a portion of this run-down is shown).

Figure 6. A simplified flow chart for the ITACA processing (after Pacor *et al.*, 2011, and Paolucci *et al.*, 2011).

Figure 7. A simplified flow chart for the PEER NGA processing (based on written commun. from R. Darragh and W. Silva and Fortran programs of N. Abrahamson).

Figure 8. A simplified flow chart for the reference processing (used for the Turkish database [Akkar *et al.*, 2010]).

Figure 9. Displacements for the Dinar record used in Figures 1 through 5 from the “reference” processing and from the ITACA and PEER NGA processing (note that the zero of the time axis starts at the beginning of the padded time series rather than the pad-stripped time series, as in the previous figures).

Figure 10. Ratios of horizontal component response spectra from ITACA (left column) and PEER NGA (right column) processing relative to the reference processing, as a function of oscillator period. There are 2714 ratios plotted in each of the graphs, most of them being close to unity (as indicated by the 5th and 95th percentile curves shown by the dashed lines). For reference, horizontal lines have been added to show ratios of 0.9 and 1.1. The x’s at the left and toward the right side of each graph show the ratios for PGA, PGV, and PGD (the statistical distributions of PGA and PGV are given in Figure 13). The upper graphs are ratios plotted as a function of period, while the bottom graphs show the ratios plotted against normalized period, defined as the oscillator period divided by the corner period of the low-cut filter.

Figure 11. Ratios of vertical component response spectra from ITACA (left column) and PEER NGA (right column) processing relative to the reference processing as a function of oscillator period. There are 1357 ratios plotted in each of the graphs, most of them being close to unity (as indicated by the 5th and 95th percentile curves shown by the dashed lines). For reference, horizontal lines have been added to show ratios of 0.9 and 1.1. The x's at the left and toward the right side of each graph show the ratios for PGA, PGV, and PGD (the statistical distributions of PGA and PGV are given in Figure 14). The upper graphs are ratios plotted as a function of period, while the bottom graphs show the ratios plotted against normalized period, defined as the oscillator period divided by the corner period of the low-cut filter.

Figure 12. Histograms of outliers in the ratio plots shown in Figures 10 and 11. An outlier is defined by any ratio less than 0.7 or greater than 1.5. Note that most of the outliers correspond to very small values of ground motion and thus will not be important in practical uses of the processed data.

Figure 13. Histograms of ratios of horizontal component response spectra from ITACA (left column) and PEER NGA (right column) processing relative to the reference processing for selected values of oscillator period normalized by the low-cut filter period, as well as for PGA and PGV. The vertical lines show the 5th, 50th, and 95th percentile values of the ratios.

Figure 14. Histograms of ratios of vertical component response spectra from ITACA (left column) and PEER NGA (right column) processing relative to the reference processing for selected values of oscillator period normalized by the low-cut filter period, as well as for PGA and PGV. The vertical lines show the 5th, 50th, and 95th percentile values of the ratios.

Figure 15. Histograms of ratios of peak acceleration as computed from the difference operators in the ITACA processing code applied to the displacement time series from the reference acceleration time series, relative to the peak acceleration of the reference acceleration time series.

Figures

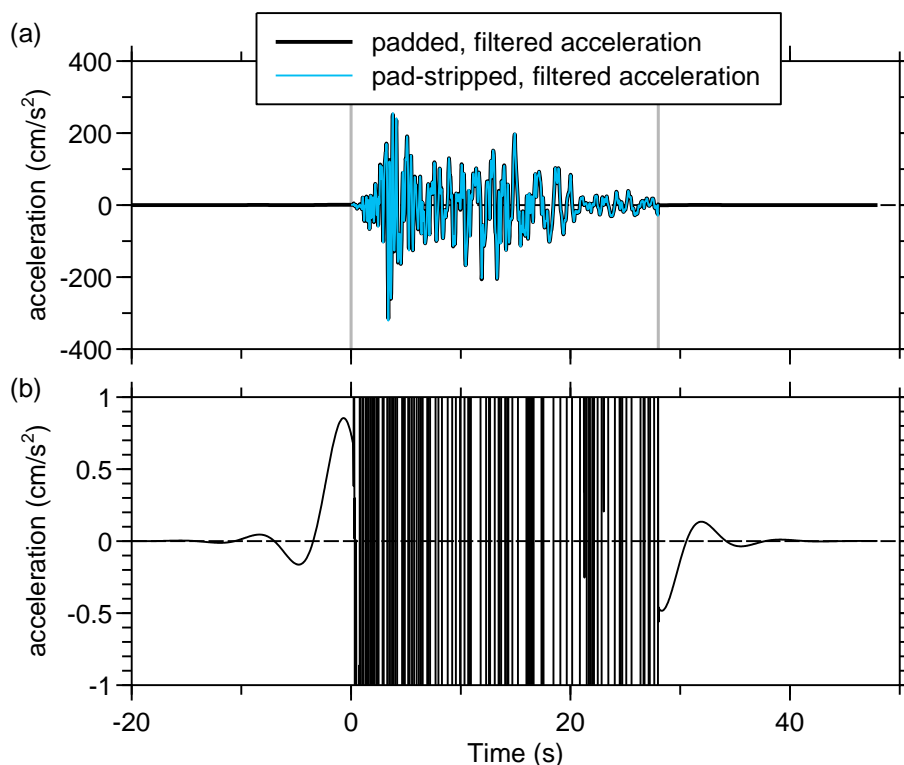


Figure 1. The acceleration time series from the Dinar recording of the 1995 Dinar earthquake after padding and filtering with an acausal low-cut filter with a corner frequency of 0.15 Hz. The thin curved line superimposed on the thick line in (a) corresponds to the time series after stripping off the padded portion. The vertical lines in the upper graph show the time limits of the original data. The vertical scale in the lower graph is expanded greatly in order to see the filter transients.

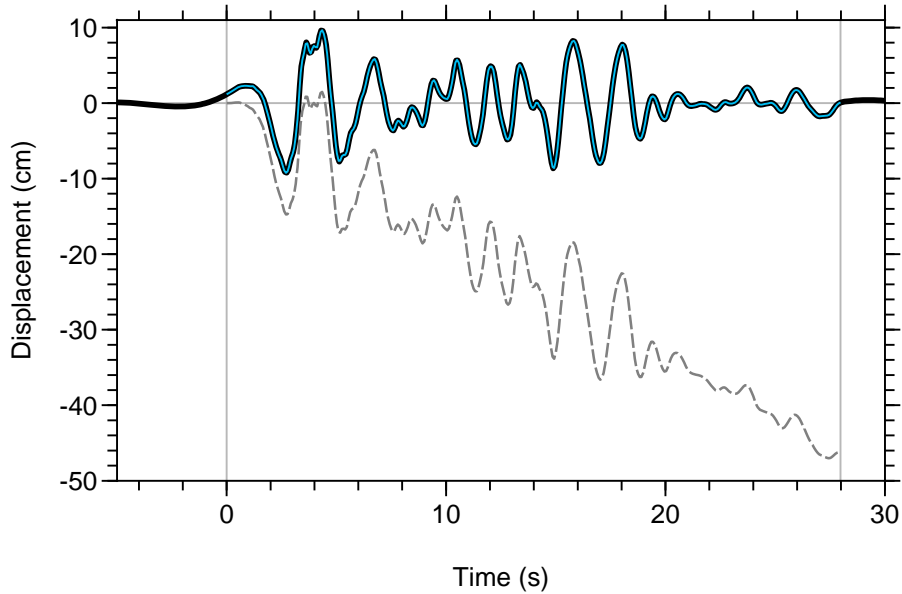
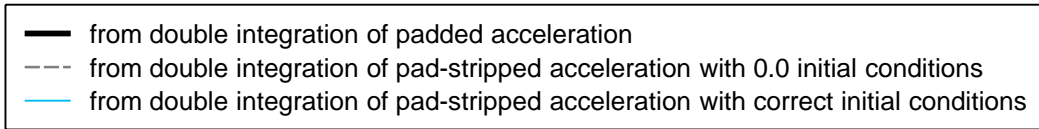


Figure 2. Displacements derived from double integration of the acceleration time series shown in Figure 1. The thick curved line is from the complete padded and filtered acceleration, whereas the dashed curve and the thin curve superimposed on the thick curved line are from integration of the pad-stripped filtered acceleration, with initial conditions for the velocity and displacement of 0.0 and the correct initial conditions, respectively.

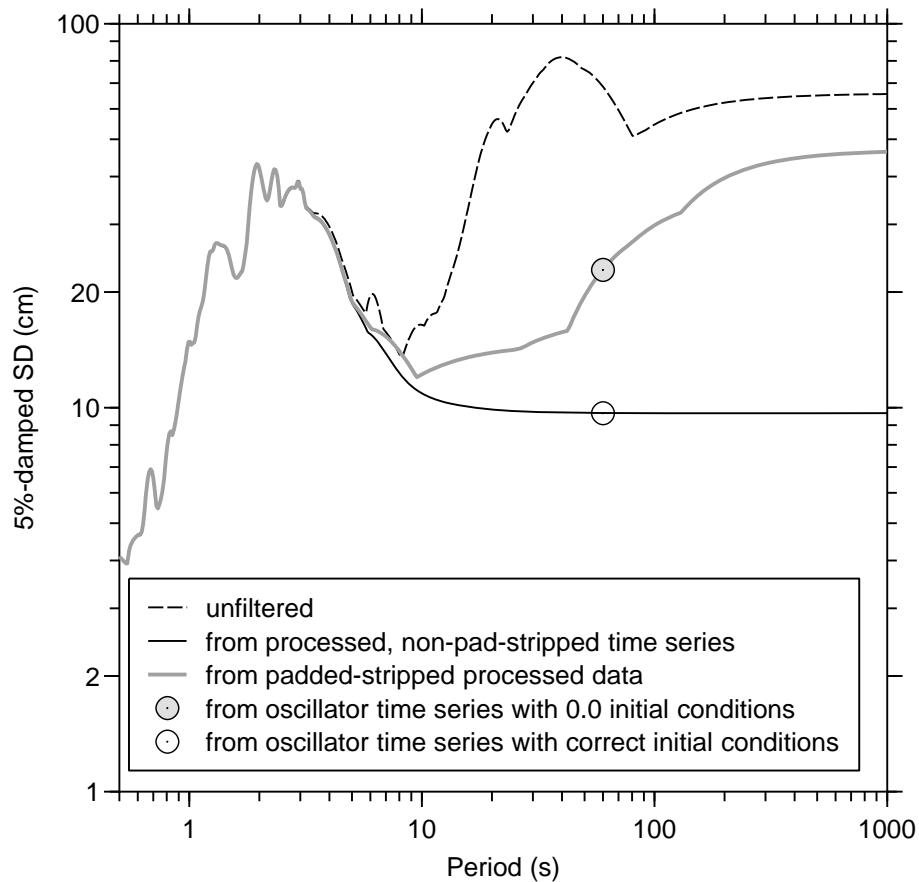


Figure 3. Response spectra computed from the unfiltered and filtered data used in the previous figures. The heavy gray curve shows the response spectrum from the time series obtained by stripping off the padded portions of the filtered acceleration time series. For all examples 0.0 was assumed for the initial oscillator displacement and velocity, except for the symbols, which were derived from oscillator time series computed from pad-stripped accelerations with different initial conditions (see text).

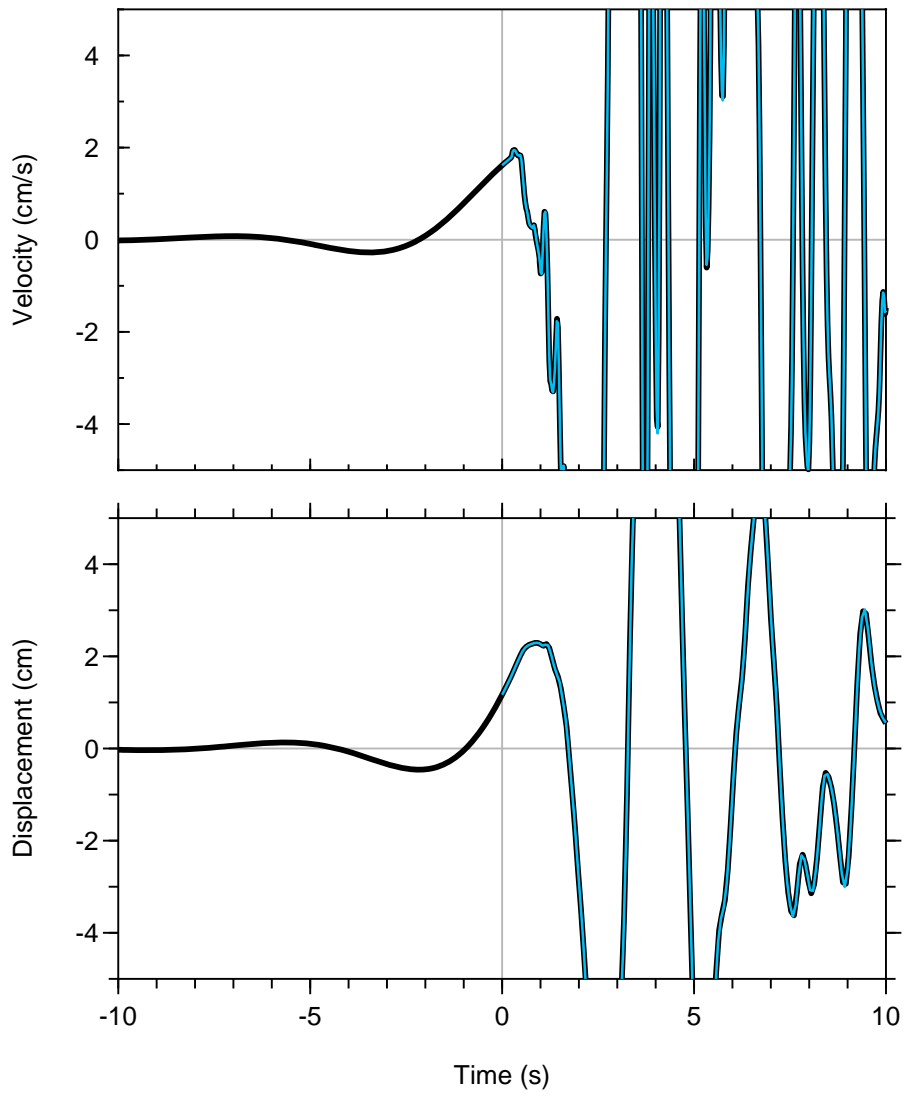


Figure 4. An expanded portion of the velocity and displacement time series derived from the padded and filtered acceleration shown in Figure 1. The curves superimposed on the thick curved lines start at the zero time of the original record and show that initial conditions of 0.0 for integration of the pad-stripped acceleration time series are incorrect.

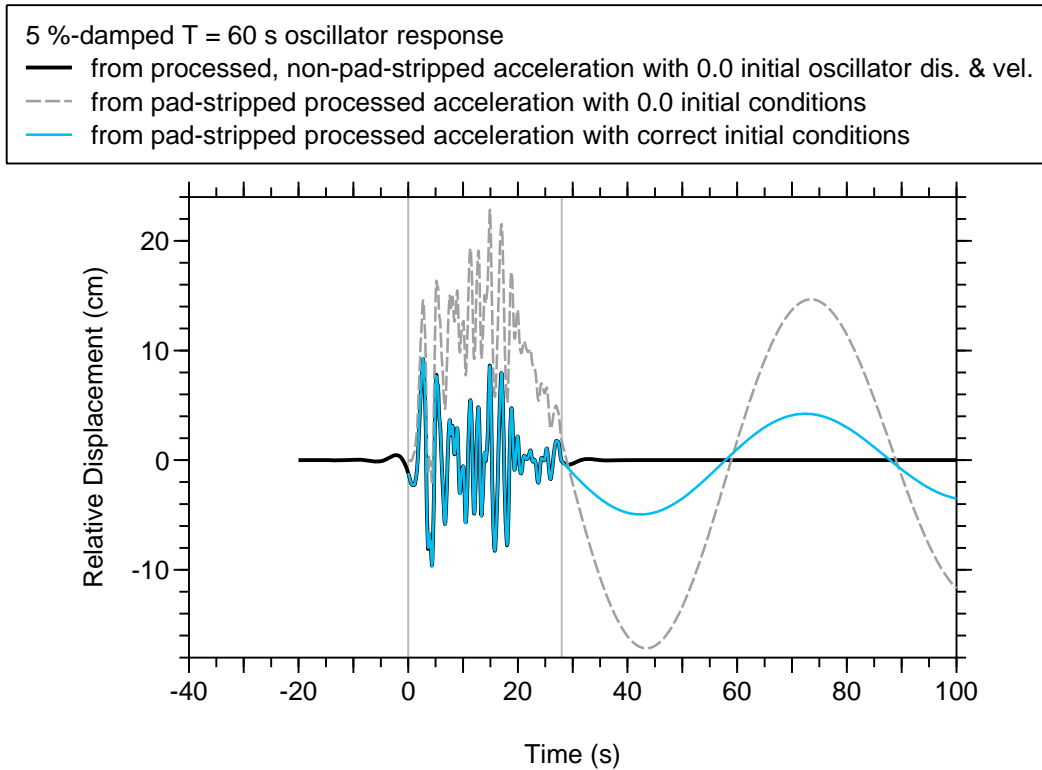


Figure 5. The $T = 60$ s oscillator response for the processed data where the padded portions were retained and were stripped off, with initial conditions as shown in the legend. The thick curved line is from the complete padded and filtered acceleration, whereas the dashed curve and the thin curve superimposed on the thick curved line are from the pad-stripped filtered acceleration with initial conditions for the oscillator velocity and displacement of 0.0 and the correct initial conditions, respectively. The vertical lines show the extent of the original record before padding; 19.995 s of zeros were added before and after the original time series, and additional zeros were added at the end of the processed time series to allow the run-down of the oscillator response (only a portion of this run-down is shown).

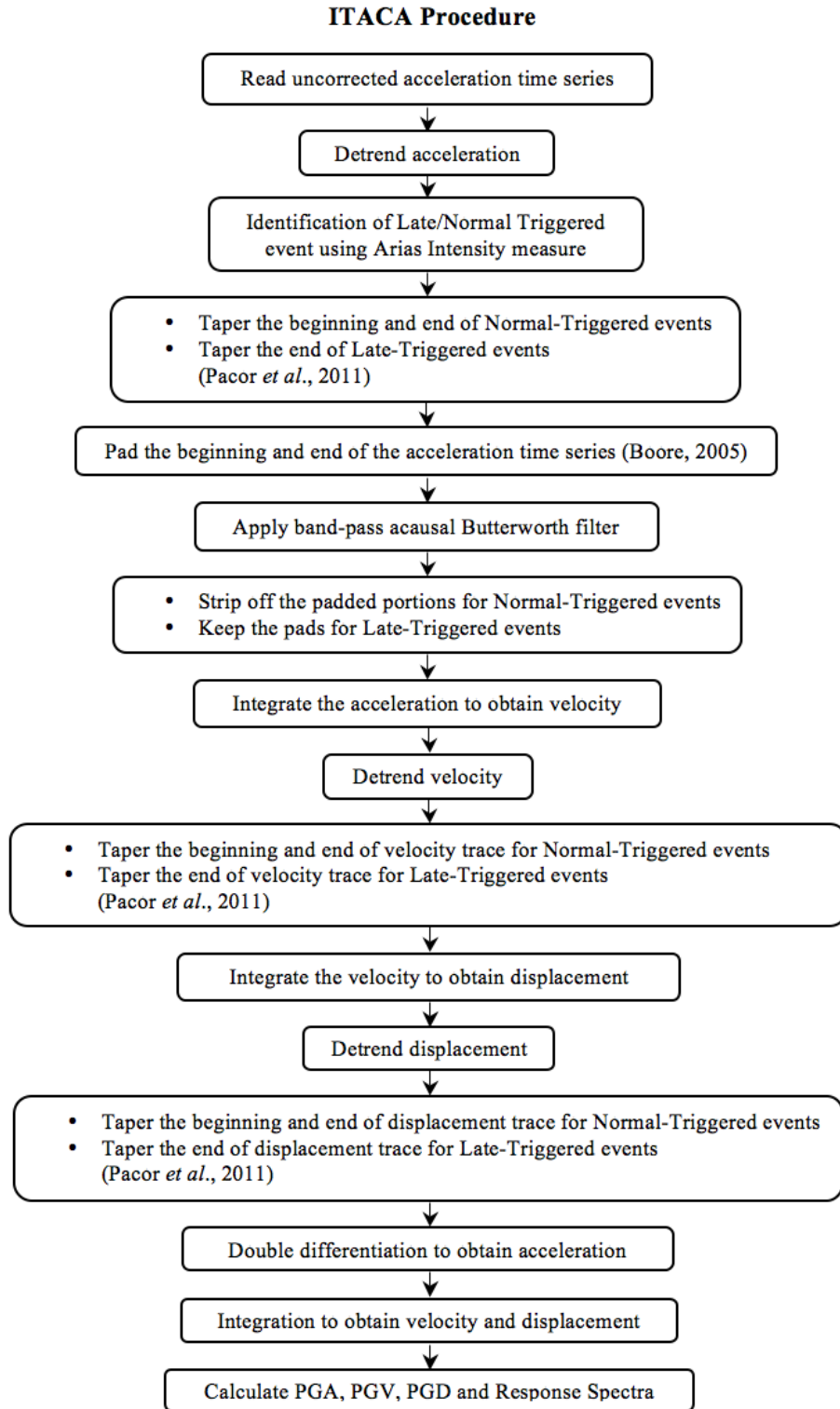


Figure 6. A simplified flow chart for the ITACA processing (after Pacor *et al.*, 2011, and Paolucci *et al.*, 2011).

PEER NGA Procedure

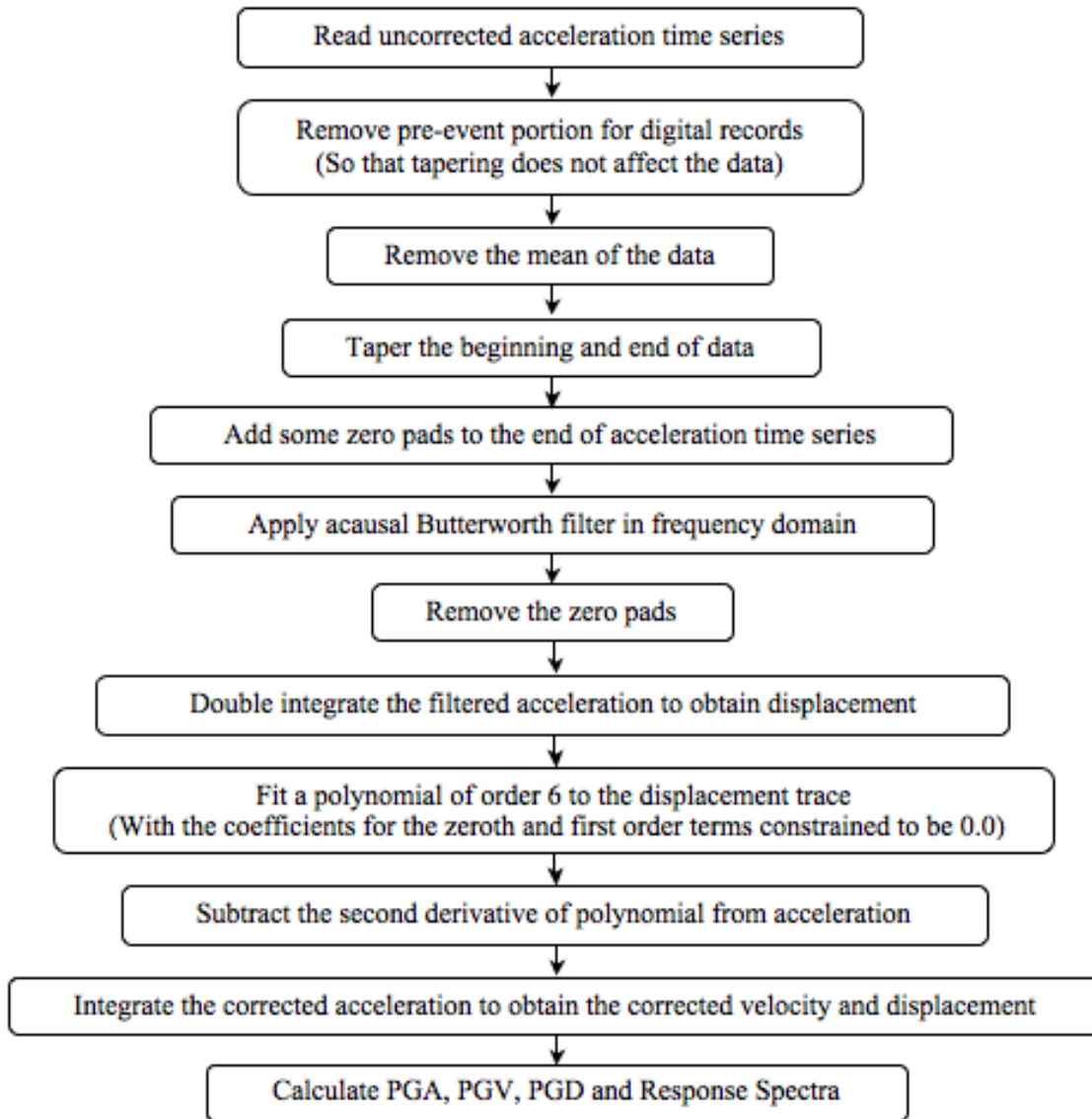


Figure 7. A simplified flow chart for the PEER NGA processing (based on written commun. from R. Darragh and W. Silva and Fortran programs of N. Abrahamson).

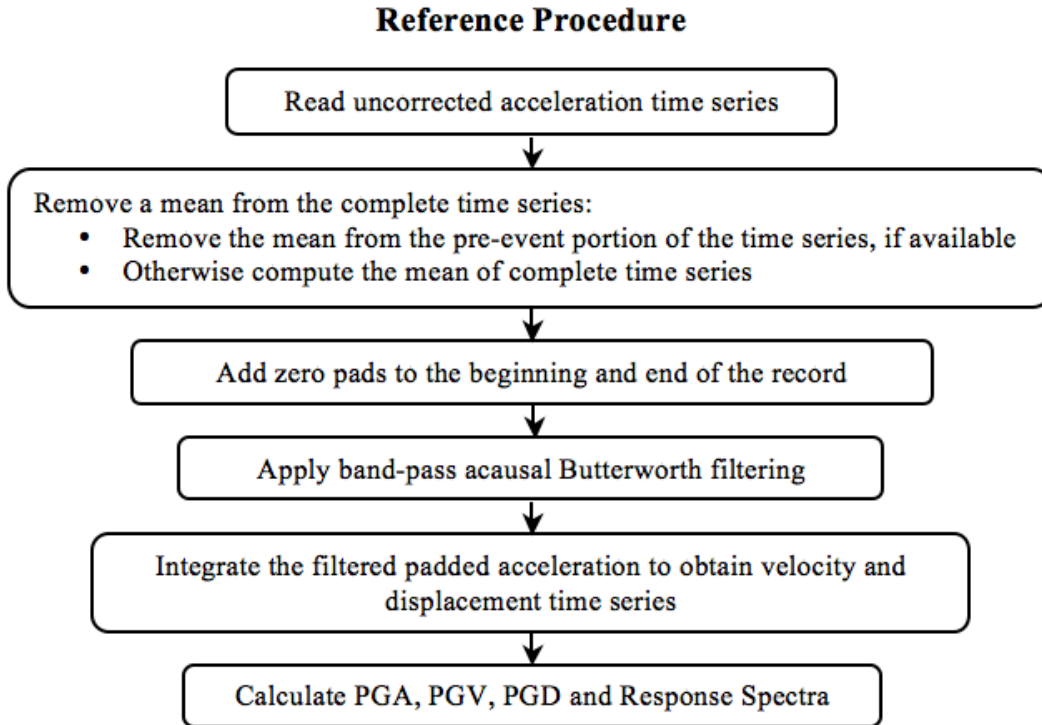


Figure 8. A simplified flow chart for the reference processing (used for the Turkish database [Akkar *et al.*, 2010]).

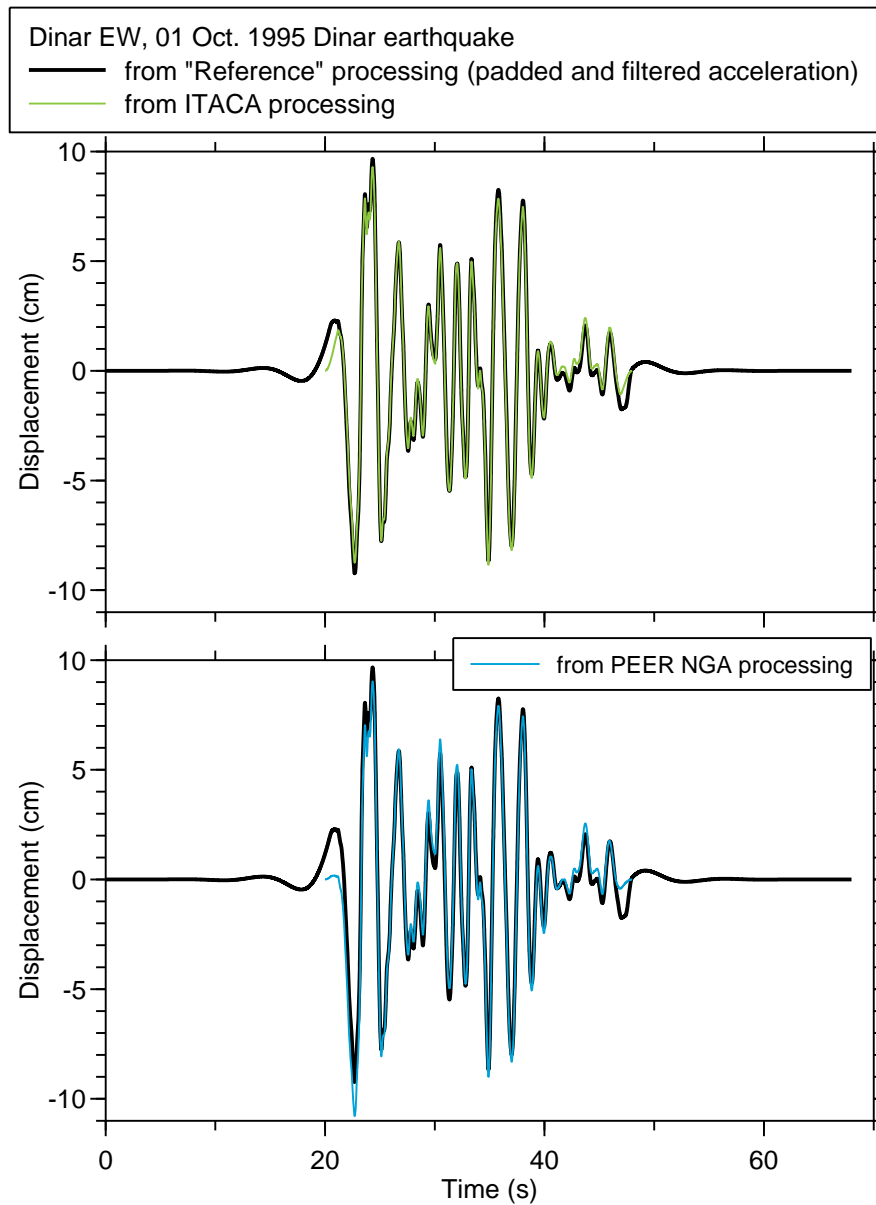


Figure 9. Displacements for the Dinar record used in Figures 1 through 5 from the “reference” processing and from the ITACA and PEER NGA processing (note that the zero of the time axis starts at the beginning of the padded time series rather than the pad-stripped time series, as in the previous figures).

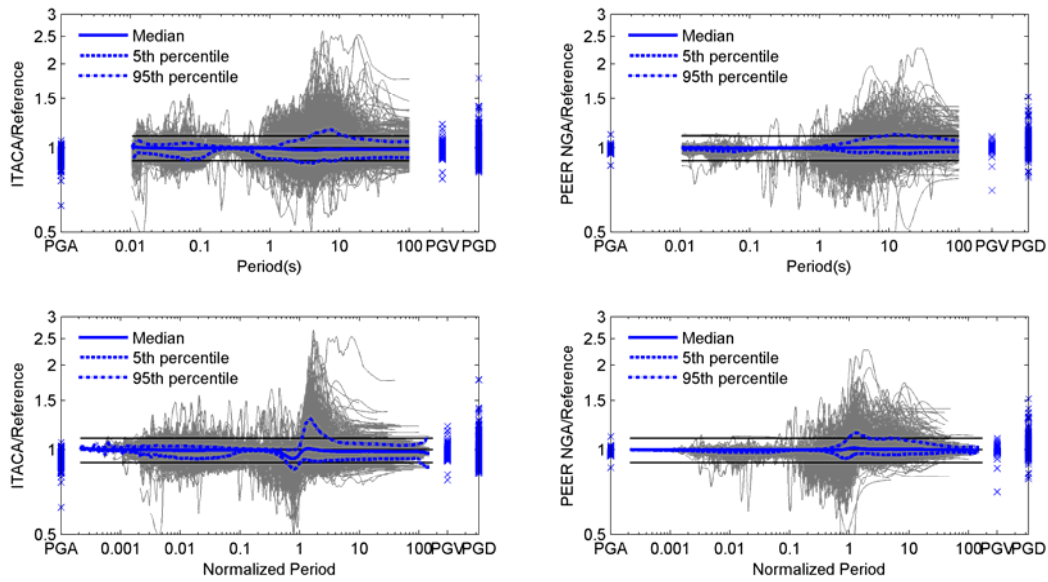


Figure 10. Ratios of horizontal component response spectra from ITACA (left column) and PEER NGA (right column) processing relative to the reference processing, as a function of oscillator period. There are 2714 ratios plotted in each of the graphs, most of them being close to unity (as indicated by the 5th and 95th percentile curves shown by the dashed lines). For reference, horizontal lines have been added to show ratios of 0.9 and 1.1. The x's at the left and toward the right side of each graph show the ratios for PGA, PGV, and PGD (the statistical distributions of PGA and PGV are given in Figure 13). The upper graphs are ratios plotted as a function of period, while the bottom graphs show the ratios plotted against normalized period, defined as the oscillator period divided by the corner period of the low-cut filter.

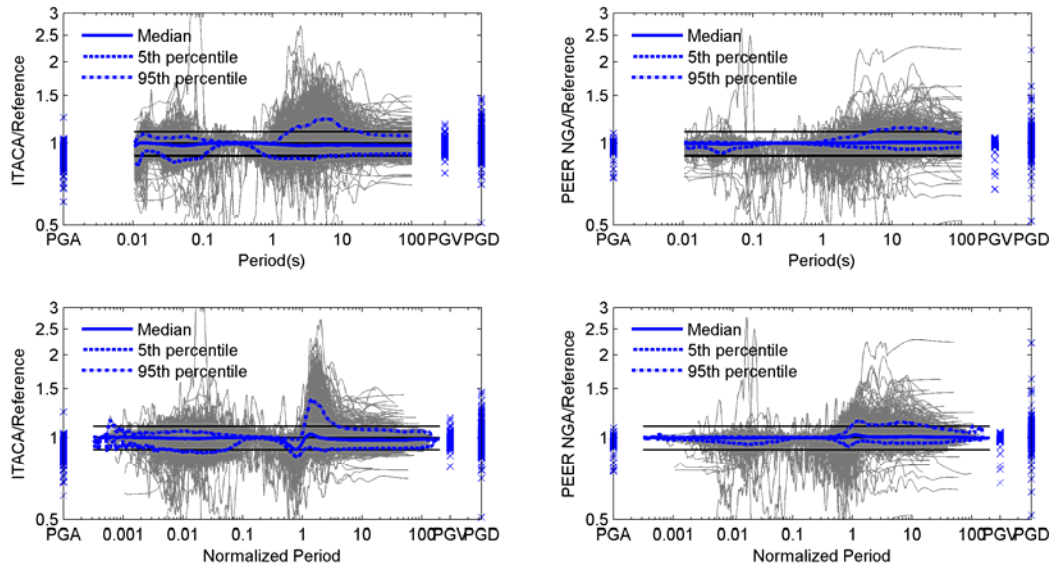


Figure 11. Ratios of vertical component response spectra from ITACA (left column) and PEER NGA (right column) processing relative to the reference processing as a function of oscillator period. There are 1357 ratios plotted in each of the graphs, most of them being close to unity (as indicated by the 5th and 95th percentile curves shown by the dashed lines). For reference, horizontal lines have been added to show ratios of 0.9 and 1.1. The x's at the left and toward the right side of each graph show the ratios for PGA, PGV, and PGD (the statistical distributions of PGA and PGV are given in Figure 14). The upper graphs are ratios plotted as a function of period, while the bottom graphs show the ratios plotted against normalized period, defined as the oscillator period divided by the corner period of the low-cut filter.

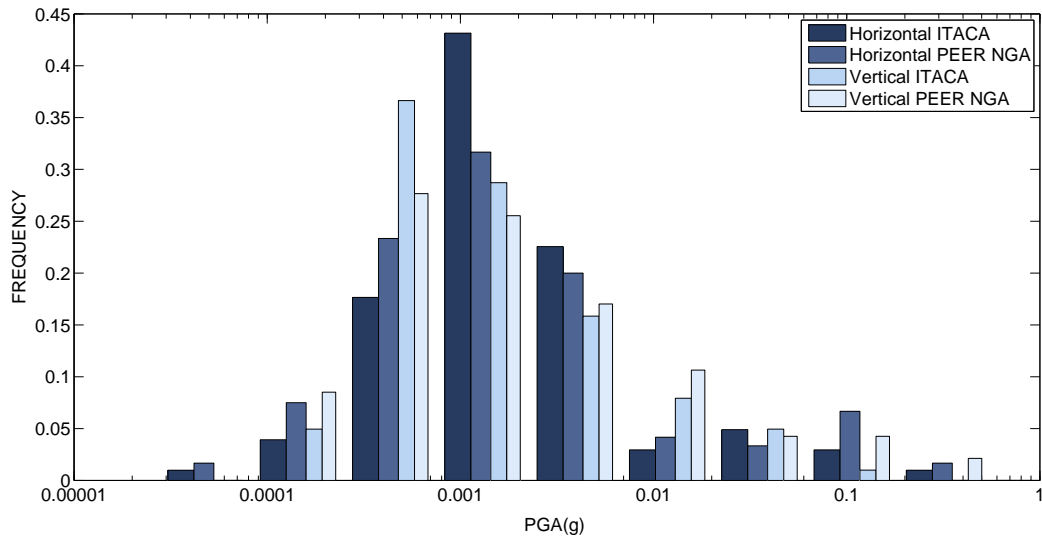


Figure 12. Histograms of outliers in the ratio plots shown in Figures 10 and 11. An outlier is defined by any ratio less than 0.7 or greater than 1.5. Note that most of the outliers correspond to very small values of ground motion and thus will not be important in practical uses of the processed data.

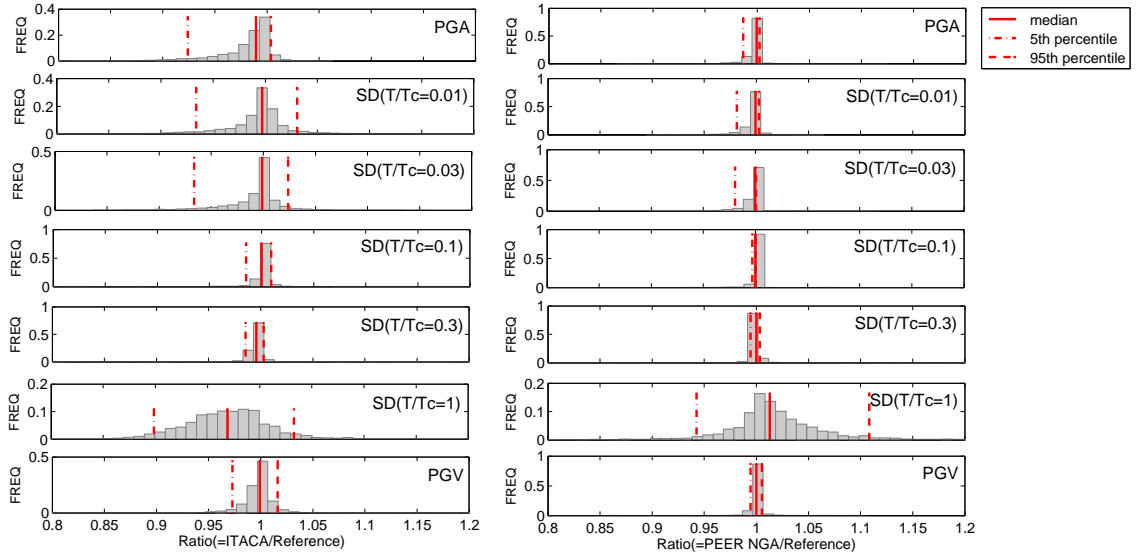


Figure 13. Histograms of ratios of horizontal component response spectra from ITACA (left column) and PEER NGA (right column) processing relative to the reference processing for selected values of oscillator period normalized by the low-cut filter period, as well as for PGA and PGV. The vertical lines show the 5th, 50th, and 95th percentile values of the ratios.

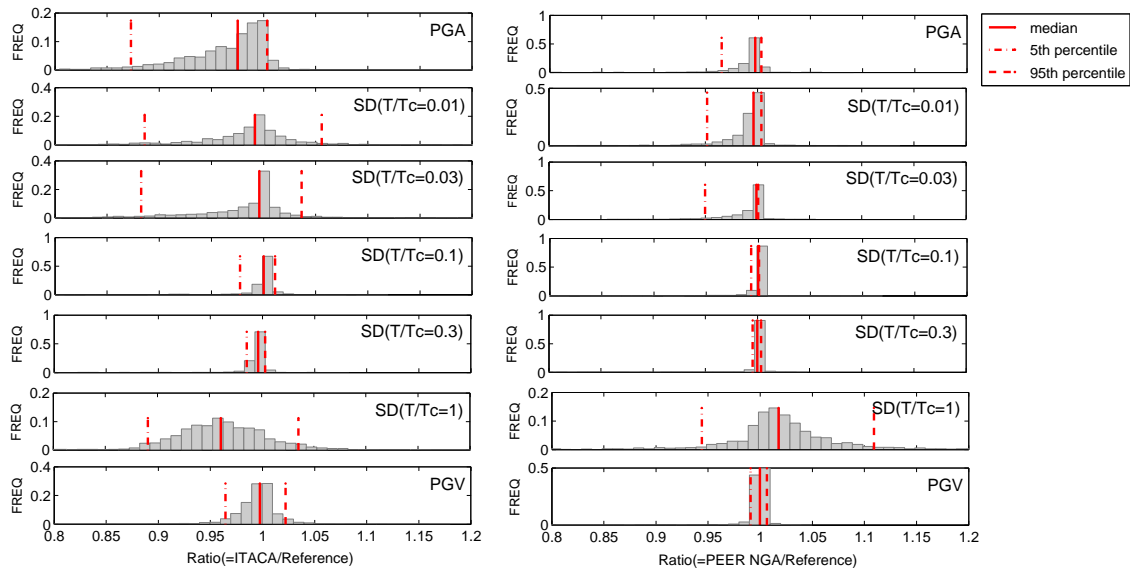


Figure 14. Histograms of ratios of vertical component response spectra from ITACA (left column) and PEER NGA (right column) processing relative to the reference processing for selected values of oscillator period normalized by the low-cut filter period, as well as for PGA and PGV. The vertical lines show the 5th, 50th, and 95th percentile values of the ratios.

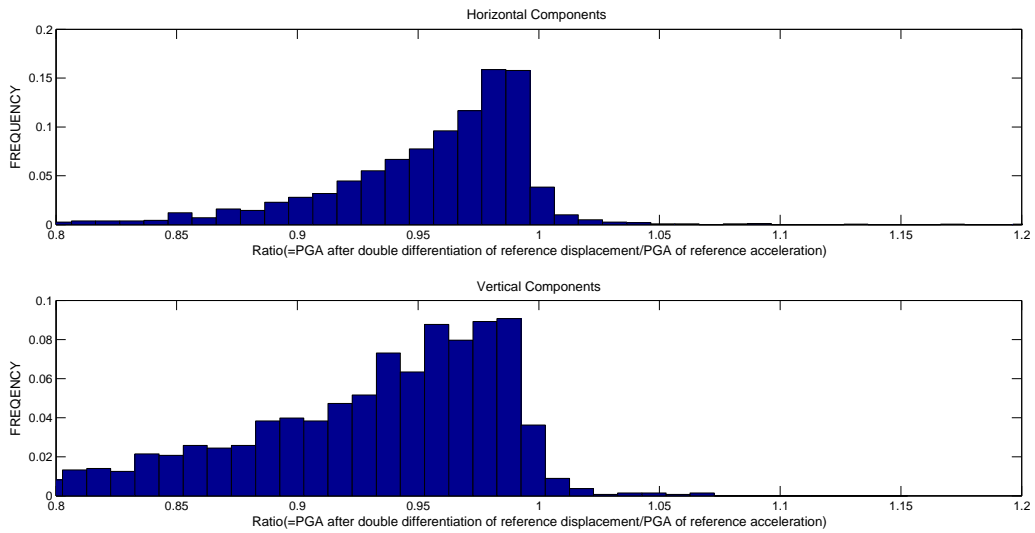


Figure 15. Histograms of ratios of peak acceleration as computed from the difference operators in the ITACA processing code applied to the displacement time series from the reference acceleration time series, relative to the peak acceleration of the reference acceleration time series.